*Korean J. of Chem. Eng.*, 3(1) (1986) 15-21

# AIR SEPARATION BY ADSORPTION ON MOLECULAR SIEVE 5A

**Il-Shik MOON, Dong-Il LEE*, Jai-Ho YANG, and Hwa-Won RYU**

Department of Chemical Engineering, College of Engineering,
Chonnam National University, Gwang-ju, Korea

*(Received 20 May 1985 • accepted 6 February 1986)*

**Abstract**— An experimental and theoretical study is given of the separation of oxygen and nitrogen in air by a single column pressure swing adsorption. Adsorption equilibrium and chromatographic experiments were also carried out to determine the adsorption parameters of the theoretical equation. The theoretical solution applied in this study with the assumption of Freundlich adsorption equilibrium has good agreement with the experimental results.

## INTRODUCTION

Pressure Swing Adsorption (PSA), which is a short cycle time adsorption/desorption process in fixed beds of adsorbent using gas pressure change as a major operating parameter, is increasingly being used for gas separation. Compared to Thermal Swing Adsorption (TSA) processes which employ two different temperature levels for adsorption/desorption, PSA processes operate at essentially isothermal conditions between two pressures and, therefore, require no heating and cooling steps [1]. Concerned with the theoretical analysis of PSA processes, quite a few articles [2-9] have been presented. And PSA technology is being applied to some industrial processes of gas separation.

For small-scale production of oxygen rich gas (up to 95%), Lee & Stahl [10] particularly stress the economic and operational advantages of PSA processes over conventional cryogenic air separation ones.

Use of molecular sieves as the adsorbents has been reported in the literatures [11-13] and the oxygen-enriched air is being extensively used for secondary sewage treatment [1] and hospitals. In that case, the enrichment of oxygen in air is due to the selective adsorption of nitrogen by quadrupole interaction between nitrogen and molecular sieve [14]. Chihara et al. [15, 16] treated molecular sieving carbons with hydrocarbons in helium gas at high temperature in order to use them as the adsorbents for air separation. The principle of their method is the preferential adsorption of oxygen by the difference of diffusion rate between oxygen and nitrogen into the treated molecular sieving carbons.

Investigations on the utilization of natural zeolites [17, 18] have been also carried out. In this study Molecular Sieve 5A was chosen as the adsorbent, which is known to be suitable for air separation among synthetic zeolites [19]. Industrial PSA systems employ several columns and complex systems of purging and pressure equalization that have been described. But this study is restricted to properties of single column operating in a three-step cycle: step 1; pressurization, step 2; product release, step 3; depressurization.

The adsorption equilibrium and chromatographic experiments were also carried out to find out the adsorption parameters in the model separately.

## THEORY

An important assumption in the model is that the gas phase composition is homogeneous in the bed. This assumption was confirmed by measuring the gas phase composition in condition of mixing the column well until equilibrium state was reached. The transfer of adsorbate in step 1 & 2 may be described by following mass balance and adsorption rate equation:

$$\text{Step 1}: W\frac{dq_i}{dt}+\varepsilon_b V\frac{dC_i}{dt}=QC_{i\ in} \tag{1}$$

$$\text{Step 2}: W\frac{dq_i}{dt}+\varepsilon_b V\frac{dC_i}{dt}=QC_{i\ in}-Q'C_i \tag{2}$$

$$\text{Rate of adsorption}: \gamma\frac{dq_i}{dt}=K_{si}a_v(q_i^*-q_i) \tag{3}$$

$$i : N_2 \text{ or } O_2$$

where $K_{si}$ can be determined by the chromatographic

* To whom all correspondence should be addressed.

experiments. If the adsorption isotherm follows the Freundlich type,

$$q_i^* = K_i C_i x_i \quad (4)$$

where $K_i$ and $x_i$ can be determined by the measurment of adsorption isotherm. In order to get the numerical solutions, the above equations are changed to the following differential equations in step 1.

$$\frac{dC_o}{dt} = \frac{K_{so}a_v}{\gamma}\left(\tau_o C_{o\ in} - \frac{W}{\varepsilon_b V}K_o C_o x_o + \frac{W}{\varepsilon_b V}q_o\right) \quad (5)$$

$$\frac{dq_o}{dt} = \frac{K_{so}a_v}{\gamma}(K_o C_o x_o - q_o) \quad (6)$$

$$\frac{dC_N}{dt} = \frac{K_{so}a_v}{\gamma}\left(\tau_o C_{N\ in} - \frac{W}{\varepsilon_b V}R_D K_N C_N x_N + \frac{W}{\varepsilon_b V}R_D q_N\right) \quad (7)$$

$$\frac{dq_N}{dt} = \frac{K_{so}a_v R_D}{\gamma}(K_N C_N x_N - q_N) \quad (8)$$

In step 2 under the condition of $Q_i = Q_i'$,

$$\frac{dC_o}{dt} = \frac{K_{so}a_v}{\gamma}\left(\tau_o C_{o\ in} - \tau_o C_o - \frac{W}{\varepsilon_b V}K_o C_o x_o + \frac{W}{\varepsilon_b V}q_o\right) \quad (9)$$

$$\frac{dq_o}{dt} = \frac{K_{so}a_v}{\gamma}(K_o C_o x_o - q_o) \quad (10)$$

$$\frac{dC_N}{dt} = \frac{K_{so}a_v}{\gamma}\left(\tau_o C_{N\ in} - \tau_o C_N - \frac{W}{\varepsilon_b V}R_D K_N C_N x_N + \frac{W}{\varepsilon_b V}R_D q_N\right) \quad (11)$$

$$\frac{dq_N}{dt} = \frac{K_{so}a_v}{\gamma}(K_N C_N x_N - q_N) \quad (12)$$

where $R_D = \dfrac{\gamma/K_{sN}a_v}{\gamma/K_{so}a_v}$, $\tau_o = \dfrac{\gamma/K_{so}a_v}{\varepsilon_b V/Q}$

The constants in the equation (1)—(12) are listed in Table 1.

By using the following initial conditions,

$t = 0$ $C_i = Q_i = 0$ in step 1

$t = t_1$ $C_i = C_{i1}$, $Q_i = Q_{i1}$ in step 2

the concentrations of adsorbates and adsorption quantities can be obtained in accordance with operating time.

In case of linear adsorption isotherm,

$$q_i^* = K_{Ai} C_i \quad (13)$$

**Table 1. Constants in the differential equations.**

| Q, cm³/sec | $K_{sN}a_v$ (p=2atm abs), g/cm³ sec cm | $K_{so}a_v$ (p=2atm abs), g/cm³ sec cm |
|---|---|---|
| 42 | 1.024 | 1.873 |
| 107 | 1.049 | 1.901 |
| 195 | 1.067 | 1.921 |

the equation (4) can be replaced with the equation (13), and the analytical solutions were obtained by Chihara et al [15, 16].

## EXPERIMENTAL

### 1. Adsorbent

The adsorbent used in the experiments was Davison Molecular Sieves type 5A (MS-5A), in the form of 8-12 mesh beads. The sieves were regenerated at 300°C under vacuum for a period of at least 3 hrs. Porosity and solid density of the adsorbent measured by Helium Pycnometer (Model SPY-1 Quantachrome Co., U.S.A.) were 0.51 and 2.28 g/cm³, respectively.

### 2. Chromatographic experiments

The apparatus is similar to that of Kaguei et al. [20] and Lee et al [21]. A 20 mm (i.d.) column made of stainless steel was used for the adsorption measurements. Helium carrier gas flowed downward first through a calming section (packed with 1.8 mm glass beads to a length of 15 cm), then through the test bed of MS-5A (packed to a length of 20 cm) and finally through an after-bed (15cm) of the same molecular sieves. A pulse of $N_2$ and $O_2$ was introduced before the calming section, and the concentrations were measured with tungsten filaments placed before and after the test bed.

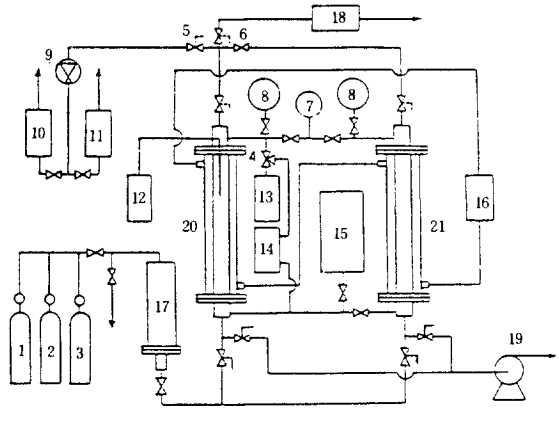


**Fig. 1. Experimental apparatus.**

1. $N_2$ cylinder
2. $O_2$ cylinder
3. Air cylinder
4. 3-way valve
5. Solenoid valve
6. Needle valve
7. Vacuum valve
8. Pressure gauge
9. Letdown valve
10. Soap flow meter
11. Rotameter
12. Thermocouple
13. Pressure transducer
14. Circulator (Gas)
15. Calibration tank
16. Circulator (Water)
17. Dryer (Silica gel)
18. Gas chromatograph
19. Vacuum pump
20. Adsorption column
21. Auxiliary column

### 3. PSA apparatus and operations

Fig. 1 shows the PSA apparatus, which was also used to measure the adsorption isotherms above the atmospheric pressure (1-7 atm abs.). The adsorption column made of stainless steel (double pipe of i.d. = 36.6 mm, o.d. = 70.0 mm and length = 500 mm) contained 373 gr of adsorbent and was maintained at a constant temperature using a thermostatically controlled water bath. Standard ¼ inch brass tubing was used throughout the system. Porous metal plates were placed at both ends of the bed to hold the packing in position, and copper-constantan thermocouple was inserted in the center of the bed to check the temperature of the bed. Adsorption isotherms of oxygen and nitrogen on MS-5A were determined by the following procedure.

After the adsorption column had reached the set temperature, the circulating system, which consisted of the auxiliary column and the interconnecting tubing, was evacuated. A quantity of gas was bled into the circulating system from the gas cylinder via a silicagel drier. The gas was then expanded into the adsorption column and left to reach equilibrium state. The initial and the final pressure were recorded. The adsorption column was then sealed off and a new dose of gas again fed to the circulating system. The gas was again expanded into the adsorption column, left to reach equilibrium state. Also the initial and the final pressure were recorded. This procedure was repeated until the final equilibrium pressure was up to 7 atm abs. One cycle operation of PSA apparatus consisted of the following three steps.

Air delivered from a commercial compressed air cylinder passed through a drying unit and was supplied to the column up to a set pressure (step 1.). The top outlet solenoid valve was opened to release the oxygen enriched air with new air being fed to the inlet to maintain the same pressure of step 1. (step 2.). The discharged gas was withdrawn at the bottom outlet and column was evacuated (step 3.). In step 1. and 2., the pressure of the bed and the concentration of product gas were continuously measured by pressure transducer (PH-A Kyowa electric instruments Co.) and gas chromatograph (Shimadzu GC-7AG), respectively. And to check the average concentration, the product gas was circulated around the column by the circulating pump until equilibrium state is reached.

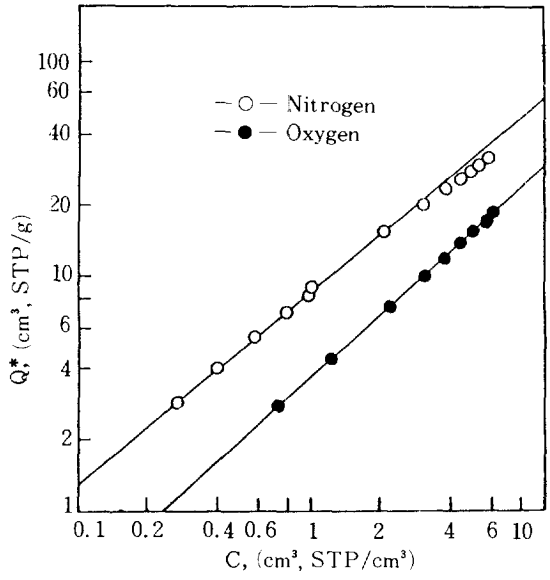


**Fig. 2. Freundlich plot from adsorption of $N_2$ and $O_2$ at 20℃ on Molecular Sieve 5A.**

## RESULTS AND DISCUSSION

### 1. Adsorption isotherms

From the experimental adsorption equilibrium data, Freundlich plot is depicted in Fig. 2. $K_i$ and $x_i$ of equation (4) can be obtained from the intercept and the slope in Fig. 2. Also from adsorption isotherms of $O_2$ and $N_2$ on MS-5A, lower temperature and pressure were expected to be a better condition to separate $O_2$ in air since $N_2$ is adsorbed much more than $O_2$ on MS-5A. The ratio of adsorption amount of $N_2$ on MS-5A to that of $O_2$ is 1.4—2.6 at the range of 0—30°C and 1—7 atm abs., which is tabulated in Table 2.

### 2. Pressure dependence of adsorption parameters

Time-domain analysis was done to find out adsorption parameters of $N_2$ and $O_2$ on MS-5A in flowing system at 25°C. The method of Lee et al. [21] was used in analyzing the response data obtained from chromatographic experiment. The $\rho_p K_A$ values shown in Fig. 3 are determined by minimizing the error between the experimental and calculated response curves.

The adsorption equilibrium constants, $K_A$, of $N_2$ and $O_2$ decrease with increasing pressure, the decreasing

**Table 2. The ratio of adsorption amount of nitrogen to that of oxygen under constant pressure, constant temperature.**

A. Constant pressure, 5 atm abs.

| Temp., ℃ | 10 | 20 | 30 | 40 |
|---|---|---|---|---|
| Ratio, $N_2/O_2$ | 1.69 | 1.64 | 1.64 | 1.61 |

B. Constant temperature, 30℃

| Pressure, atm abs. | 2 | 3 | 4 | 5 |
|---|---|---|---|---|
| Ratio, $N_2/O_2$ | 1.84 | 1.70 | 1.64 | 1.50 |

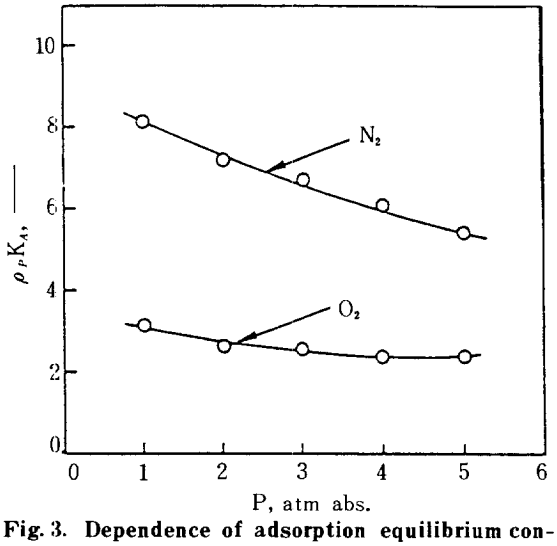


**Fig. 3. Dependence of adsorption equilibrium constant on pressure.**

rate of $N_2$ being higher than that of $O_2$ (Fig. 3 ). Therefore, the degree of separation was expected to decrease with increasing pressure, which agrees with the results of the adsorption equilibrium experiments.

Using the determined value of $K_A$, the relation of axial dispersion coefficient, $D_{ax}$, and intraparticle effective diffusivity, $D_e$, is computed for each run. Fig. 4 is the error map about the adsorption system of $N_2$ and $O_2$ on MS-5A at 4 atm abs. In laminar flow range, $D_{ax}$ is considered not to depend upon the flow rates, so that the $D_{ax}$ and $D_e$ can be determined from where all the contours overlap.

The $D_e$ values determined at each pressure also decrease with increasing pressure (Fig. 5 ), which shows the same results as the Kawazoe's [22]. Overall mass transfer coefficient, $K_s a_v$, was calculated from the following equation.

$$\frac{1}{K_s a_v} = \frac{1}{k_s a_v} + \frac{K_A}{k_f a_v} \tag{14}$$

where $k_s a_v$ was determined from $D_e$ and $K_A$ [19], $k_f a_v$ from the equation [23] proposed by Wakao et al. The overall mass transfer coefficient decreases with increasing pressure for both $N_2$ and $O_2$, which is tabulated in Table 3.

### 3. Enrichment of $O_2$ in air by PSA method

PSA experiments were done at four feed flow rates: 42, 47, 107 and 195 $cm^3$/sec and at two pressures: 2 and

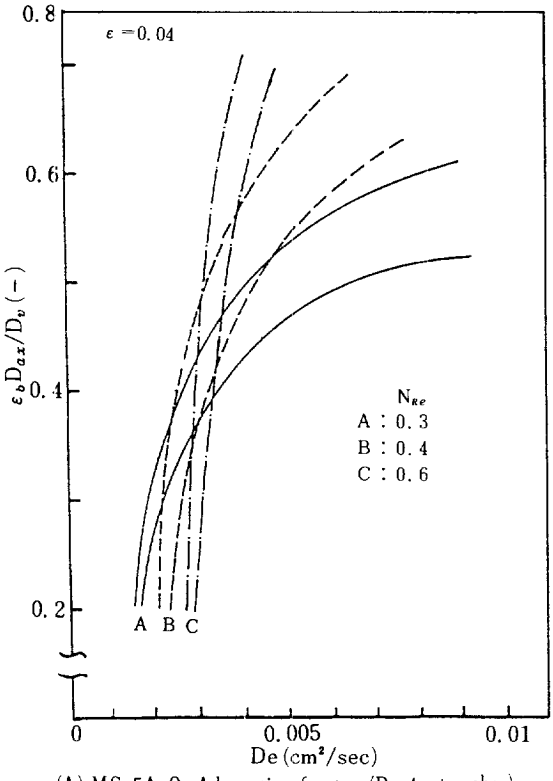


(A) MS 5A-$O_2$ Adsorption System (P=4 atm abs.)

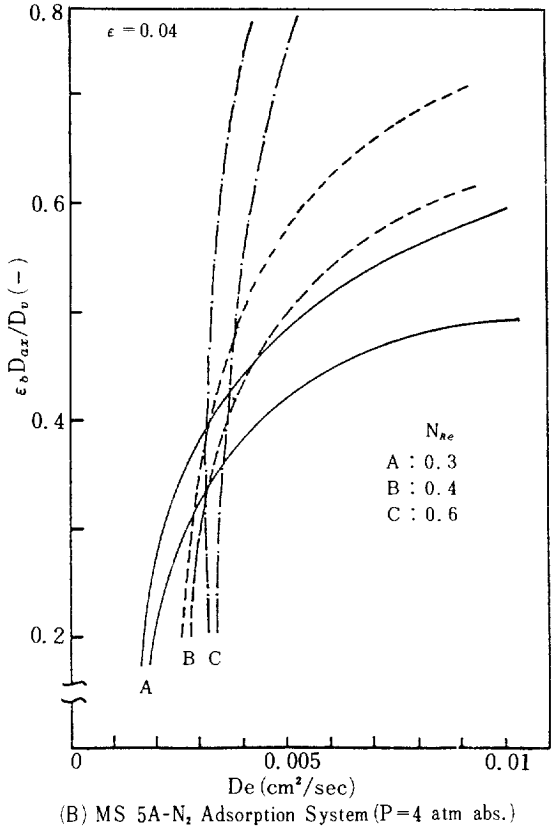


(B) MS 5A-$N_2$ Adsorption System (P=4 atm abs.)

**Fig. 4. Error map in plot of $\varepsilon_b D_{ax}/D_v$ vs. $D_e$.**

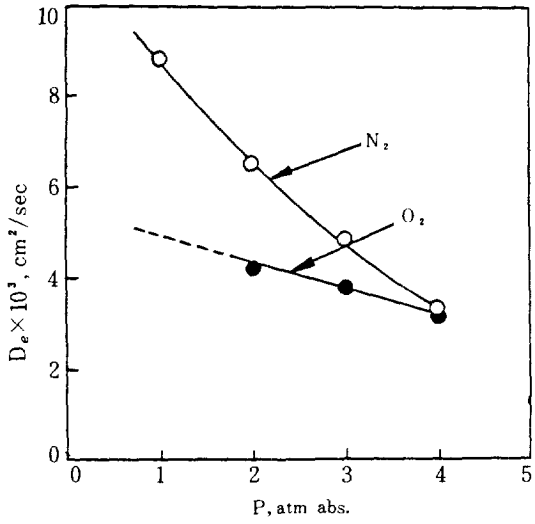


**Fig. 5. Dependence of effective diffusivities on pressure.**

**Table 3. The relation between overall mass transfer coefficient (g/cm²·sec) and pressure.**

| gas \ p, atm abs. | 1 | 2 | 3 | 4 |
|---|---|---|---|---|
| $O_2$ | 0.2837 | 0.1687 | 0.1543 | 0.1383 |
| $N_2$ | 0.1133 | 0.0919 | 0.0178 | 0.0561 |

3 atm abs. The exit and average concentrations of the column were measured respectively.

The theoretical oxygen concentrations calculated from the different flow rates and pressures are summarized graphically in Fig. 6 and 7. Fig. 6 represents that the enriched oxygen concentration at the start of

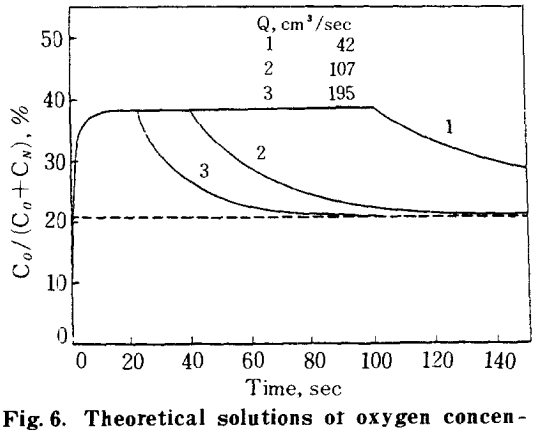


**Fig. 6. Theoretical solutions of oxygen concentration with variation of flow rates: 2 atm abs., 25℃, $K_{AN}$=6.55 cm³/g.**

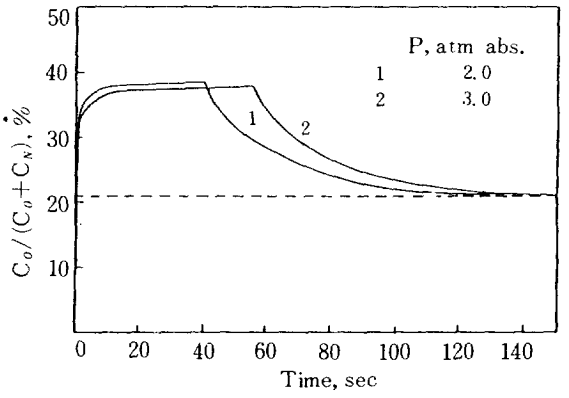


**Fig. 7. Theoretical solutions of oxygen concentration at 25℃: $K_{AN}$=6.55 cm³/g, $K_{AO}$=2.40 cm³/g, Q=107 cm³/sec.**

step 2 is scarcely influenced by the flow rate under the constant pressure. However, the oxygen concentration at 3 atm abs. is a little lower than that at 2 atm abs. in Fig. 7. This corresponds with the fact that the ratio of ($N_2$ amount adsorbed)/($O_2$ amount adsorbed) and that of $K_{AN}/K_{AO}$ decreased with increasing pressure. In order to see the effect of adsorption equilibrium constant on the degree of separation, $K_{AN}$ was changed under the constant $K_{AO}$.

As shown in Fig. 8 the calculated maximum average concentration is 38.8, 44 and 50% with the variations of $K_{AN}$ respectively. This shows the larger ratio of $K_{AN}$ to $K_{AO}$ is the condition of the better separation of air, as would be expected.

Generally as the adsorption process progresses, adsorption zones are formed and the concentration of ad-

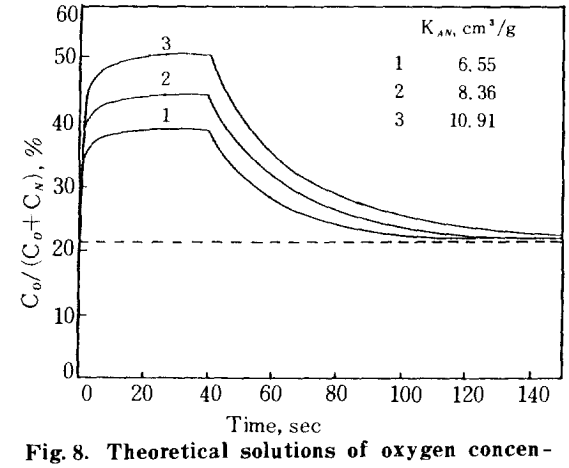


**Fig. 8. Theoretical solutions of oxygen concentration with variation of $K_{AN}$: 2 atm abs., 25℃, Q=107 cm³/sec.**

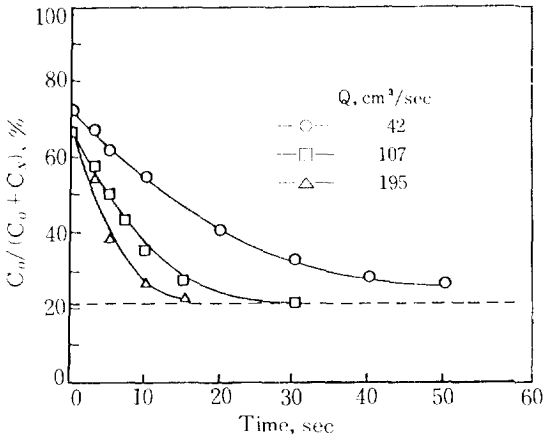


**Fig. 9. Oxygen concentration at outlet of column in step 2: 2 atm abs., 25℃.**

sorbate varies vertically in bed. So the $O_2$ concentration at the exit of column will be richer than the average concentration where the adsorbate composition is homogeneous in the bed. The effect of adsorptions on the product concentration is shown in Fig. 9 and 10, where the runs were made at not-mixing condition.

To ensure a valid comparison with the model, the average concentrations of the bed were measured. The experimental results and the theoretical calculations are compared in Fig. 11, 12 and 13. Considering possible experimental errors, it can be considered that the experimental results agree well with theoretical ones. Particulary the assumption of Freundlich type had better agreement than that of linear type.

Oxygen yield, (average $O_2$ concentration of the product)×(Amount of product)/(0.21)×(amount of the inlet air), was about 52% when the average $O_2$ concentration of product was 50%, and was nearly constant with various flow rates of 42-195 cm³/sec in Fig 14.

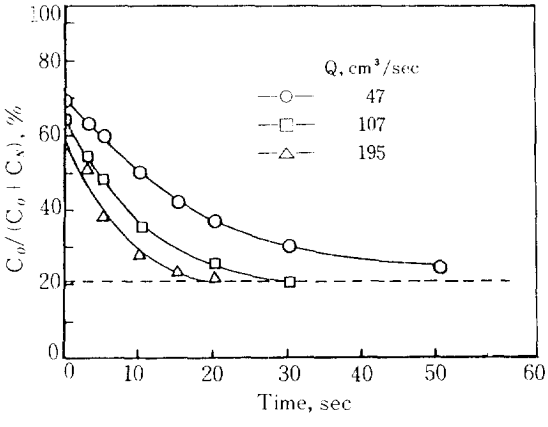


**Fig. 10. Oxygen concentration at outlet of column in step 2: 3 atm abs., 25℃.**

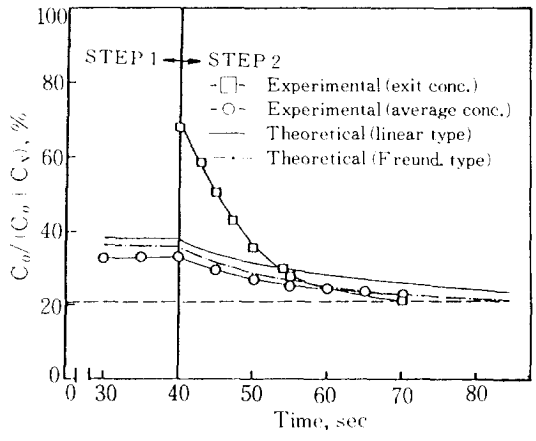


**Fig. 11. Oxygen concentration vs. time at 2 atm abs.: 25℃, $K_{AN}$=6.55, Q=42 cm³/sec.**

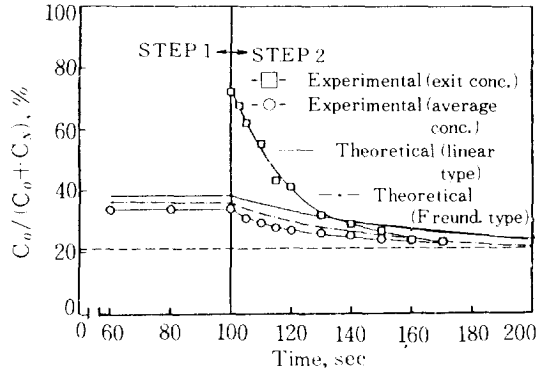


**Fig. 12. Oxygen concentration vs. time at 2 atm abs.: 25℃, $K_{AN}$=6.55, Q=107 cm³/sec.**

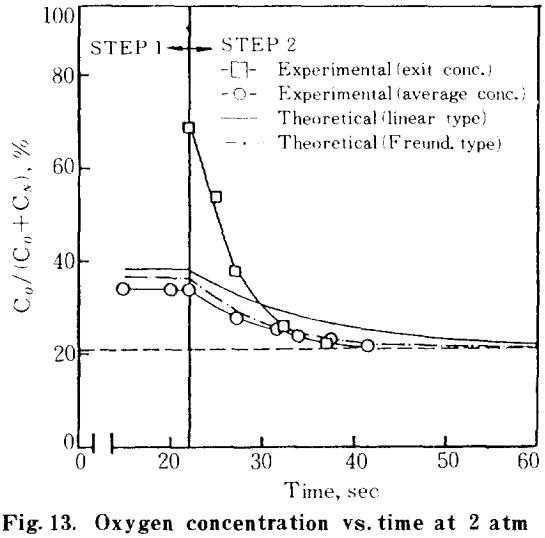


**Fig. 13. Oxygen concentration vs. time at 2 atm abs.: 25℃, $K_{AN}$=6.55, Q=195 cm³/sec.**

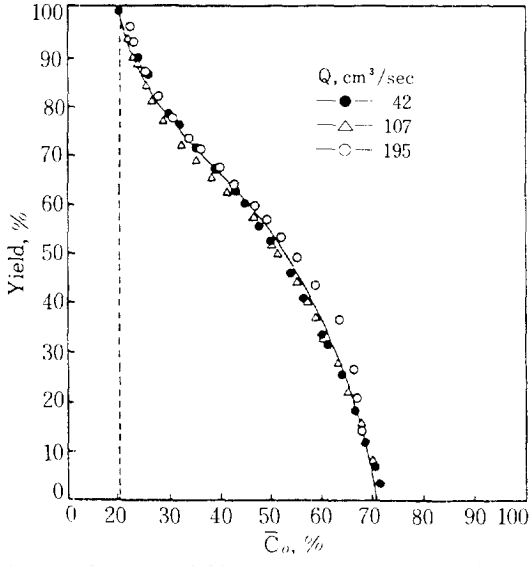


**Fig. 14. Oxygen yield vs. oxygen concentration of the product($\bar{C}_o$).**

## CONCLUSION

1. Adsorption equilibrium constant and intraparticle effective diffusivity decrease with increasing pressure.
2. Experimental results show good agreement with theoretical solutions for PSA with the assumption of Freundlich type adsorption equilibrium.

## NOMENCLATURE

$a_v$ : surface area of particle per unit volume, $cm^2/cm^3$
$C_i$ : concentration of i-component, $cm^3/cm^3$
$D_{ax}$ : axial dispersion caefficient, $cm^2/sec$
$D_e$ : effective diffusivity in a particle, $cm^2/sec$
$D_v$ : molecular diffusivity, $cm^2/sec$
$K_{Ai}$ : adsorption equilibrium constant of i-component, $cm^3/g$
$K_i$ : coefficient of i-component in Freundlich isotherm, $cm^3/g$
$K_{si}$ : overall mass transfer coefficient of i-component, $g/cm^2 \cdot sec$
$k_s$ : film mass transfer coefficient, cm/sec
$k_f$ : intraparticle mass transfer coefficient, cm/sec
P : pressure, atm abs.
Q : feed flow rate, $Ncm^3/sec$
Q′ : product flow rate, $Ncm^3/sec$
$q_i, q_i^*$ : amount adsorbed and amount adsorbed at saturation of i-component, $Ncm^3/g$
t : time, sec
T : temperature, K
V : volume of adsorption column, $cm^3$
W : amount of adsorbent, g
$x_i$ : coefficient of i-component in Freudlich isotherm
$\varepsilon$ : error
$\varepsilon_b$ : void fraction of bed
$\gamma$ : packing density, $g/cm^3$
$\rho_p$ : apparent particle density, $g/cm^3$

**Subscripts**

$n$ : nitrogen
$o$ : oxygen

## REFERENCES


1. Breck, D.W.: "Zeolite Molecular Sieves", John Wiley & Sons. New York (1974).
2. Turnock, P.H. and Kadlec, R.H., *AIChE*, **17,** 335 (1971).
3. Shendalman, L.H. and Mitchell, J.E. *Chem. Eng. Sci.*, **27,** 1449 (1972).
4. Kawazoe, K. and Kawai, T., *Kagaku Kogaku*, Japan, **37,** 288 (1973).
5. Kowler, D.E. and Kadlec, R.H., *AIChE*, **18,** 1207 (1972).
6. Chan, Y.N. and Wong, Y.M., *Chem. Eng. Sci.*, **36,** 245 (1981).
7. Carter, J.W. and Wysznski, M.L., *Chem. Eng. Sci.*, **38,** 1093 (1983).
8. Chihara, K. and Suzuki, M., *J. Chem. Eng.*, Japan, **16,** 53 (1983).
9. Nakao, S. and Suzuki, M., *J. Chem. Eng.*, Japan, **16,** 330 (1983).
10. Lee, H.J. and Stahl, D.E., *AIChE* Symposium Series, **69,** 134 (1973).
11. Bandouin, Y., Simonet, G., Eluard, R. and Pivard, C., *Chem. Abstr.*, 49645e, 80 (1974).
12. Sarnes, R., *Chem. Abstr.*, 101652, 76 (1972).
13. Pae, Y.R., Ryu, J.H., and Lee, W., *Chem. Abstr.*, 47681g, 76 (1972).
14. Barrer, R.M., *J. Colloid and Interface Science*, **21,** 417 (1966).
15. Chihara K., Suzuki, M. and Kawazoe, K., Presented at 12th autumn meeting, Soc. of Chem. Eng., Japan, G8-311 (1978).
16. Chihara, K. and Suzuki, M., *Separation Techniques*, Japan, **12,** 2 (1982).
17. Nisida, K., *Separation Techniques*, Japan, **13,** 66 (1983).
18. Ayao, T. and Yoshihiro, M., *Hun Sai*, Japan, **26,** 12 (1982).
19. Suzuki, K. and Kitagawa, H., "Pressure Swing Cycle System", Kodansa, Tokyo (1983).
20. Kaguei, S., Matsumoto, K. and Wakao, N., *Chem. Eng. Sci.*, **35,** 1809 (1980).
21. Lee, D.I. and Ryu, H.W., *Hwahak Konghak* **19,** 95(1981).
22. Kawazoe, K. and Kawai, T., *Kagaku Kogaku*, Japan, **36,** 71 (1972).
23. Wakao, N. and Funazkri, T., *Chem. Eng. Sci.*, **33,** 1375 (1978).